ABDOMINAL IMAGING

Iran J Radiol. 2018 October; 15(4):e64819. doi: 10.5812/iranjradiol.64819.

Published online 2018 July 10. **Case Report**

# Imaging Findings of Retroperitoneal Primary Extraskeletal Mesenchymal Chondrosarcoma: A Case Report

Guyi Wang [1], Zhenhua Zhao [2], Jianguo Wei [3] and Jianfeng Yang [2, *]

[1]Department of Ultrasound, Shaoxing People's Hospital (Shaoxing Hospital of Zhejiang University), Shaoxing, China
[2]Department of Radiology, Shaoxing People's Hospital (Shaoxing Hospital of Zhejiang University), Shaoxing, China
[3]Department of Pathology, Shaoxing People's Hospital (Shaoxing Hospital of Zhejiang University), Shaoxing, China

[*]*Corresponding author*: Jianfeng Yang, Department of Radiology, Shaoxing People's Hospital (Shaoxing Hospital of Zhejiang University), 568 Zhongxing North Rd, Shaoxing 312000, Zhejiang, China. Tel: +86-057588228556, Fax: +86-057588228558, E-mail: yjfnjy2002@126.com

**Received** 2017 December 05; **Revised** 2018 April 04; **Accepted** 2018 April 17.

**Abstract**

Imaging knowledge regarding retroperitoneal primary extraskeletal mesenchymal chondrosarcoma (ESMC) is limited. We report a new case of ESMC originated from the retroperitoneum. The tumor was indicated a well-defined mass with marker calcification, the parenchyma showed gradual enhancement pattern on the biphasic enhanced computed tomography and wash-in-wash-out enhancement pattern on the contrast-enhanced magnetic resonance imaging and hyperintensity on diffusion-weighted imaging which implying the dense cellularity of tumor cells. Sonography indicated an increased echogenicity nodular area in the mass. These imaging features further enriched the imaging knowledge of this rare tumor and presented valuable imaging characteristics to diagnose retroperitoneal primary ESMC.

*Keywords:* Retroperitoneum, Mesenchymal, Chondrosarcoma, Computed Tomography, X-Ray, Contrast-Enhanced, Magnetic Resonance Imaging

## 1. Introduction

The histological subtypes of chondrosarcomas include well-differentiated, mesenchymal and myxoid (1). Mesenchymal chondrosarcomas are more aggressive tumors accounting for 1 - 3% of all chondrosarcomas (2). Approximately 30 - 50% of mesenchymal chondrosarcomas occur in extraskeletal locations and commonly arise in the lower extremities (3); they rarely occur in the retroperitoneum. Knowledge regarding imaging of primary extraskeletal mesenchymal chondrosarcoma (ESMC) in the retroperitoneum is limited, and only a few reports have described computed tomography (CT) findings of different shapes of calcification and low-attenuated necrotic areas in the mass, with mild enhancement in the periphery of the mass (1, 4, 5). To our knowledge, the overall imaging features of common imaging methods including biphasic enhanced CT, diffusion-weighted imaging, multiphase contrast-enhanced magnetic resonance imaging (MRI), and sonography are incompletely understood. We provide a new case of primary ESMC in the retroperitoneum and present more detailed and valuable imaging findings to enrich the imaging knowledge concerning this tumor.

## 2. Case Presentation

A 31-year-old woman was admitted to our hospital with a mass showing an increased echogenicity nodular area in the peritoneal cavity by ultrasound following routine health examination (Figure 1). The patient denied significant medications or any symptoms and medical history. Mild left epigastric tenderness on deep palpation without rebound was found on physical examination. All laboratory data were within normal limits. The ethical approval and patient informed consent was waived by the local institutional review board.

An abdomen CT (BrightSpeed 16, GE Healthcare, Milwaukee, America) demonstrated a lobulated shaped and well-circumscribed mass measuring 5.6 × 4.3 × 4.2 cm in the left perirenal space. The lesion showed homogeneous iso-attenuation similar to that of the paraspinal muscle with nodular calcification on a plain scan (Figure 2A). After contrast agent administration (iopromide, 300 mg iodine/ml; Ultravist 300, Schering, Berlin, Germany), the parenchyma of the mass displayed evident enhancement in the arterial phase and vivid enhancement in the portal phase. The CT values of the parenchyma on the plain scan, arterial, and portal phase were 43.5 Hounsfield units (HU),

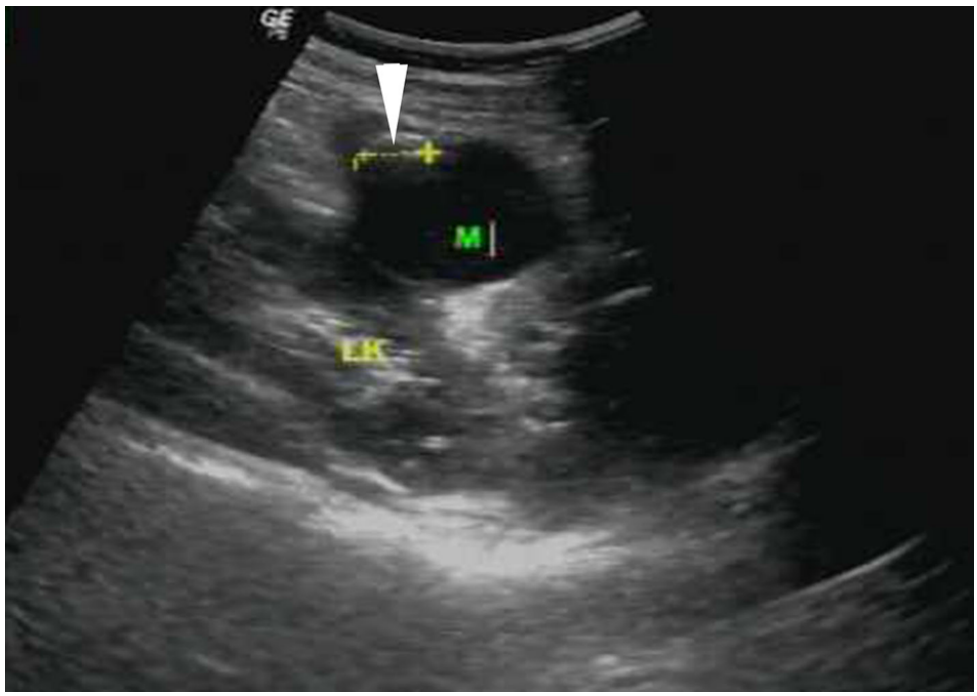


**Figure 1.** The sonography performed for a 31-year-old woman indicates an increased echogenicity nodular area (white arrowhead) in the mass.

112.7 HU, and 149.4 HU, respectively (Figures 2B and 2C). An irregular hypoattenuation area was indicated on both the arterial phase and portal phase. The adjacent left renal region was compressed but not displaced.

The parenchyma in the lesion was predominantly heterogeneously hyperintense on T2-weighted images (T2WI) and iso-hypointense on T1-weighted images (T1WI) (3T Siemens Magnetom Verio, Erlangen, Germany) (Figures 3A and 3B). There was nodular hypointensity in the interior of the mass on both T2WI and T1WI (Figures 3A and 3B). Particularly, the parenchyma was evidently hyperintense on diffusion-weighted imaging (DWI) (b value = 800) (Figure 3C) and hypointense on the apparent diffusion coefficient (ADC) map. This imaging characteristic implied that water diffusion in the parenchyma was restricted. After administration of the intravenous gadolinium contrast agent (gadopentetate dimeglumine; Bayer Schering Pharma AG, Berlin, Germany), the noncalcified area of the mass was indicated quickly, with vivid enhancement in the early arterial phase, portal phase, and contrast agent wash out in the equilibrium phase (Figures 3D-3F), and the edge of the calcific area showed moderate central enhancement (Figures 3E and 3F). The mass had a boundary with the left kidney. Lymphadenopathy was not present in the abdomen.

Laparoscopic resection of the retroperitoneal tumor was performed, and one 5.5 × 4.0 × 4.0 $cm^3$ mass was identified in the left perirenal space. The mass adhered to the left kidney envelope and peritoneum, and there was some vasa vasorum under the tumor. Macroscopically, the incisal surface of the mass specimen was grayish-red with an exquisite texture. Hematoxylin-eosin (HE) staining showed that the well differentiated cartilaginous tissue zone was surrounded by dense ovoid hyperchromatic cellularity with a confluence transition (Figure 4A). The tumor cells presented a solid and patchy growth pattern along with gross neovascularization and were arranged similar to that in the hemangiopericytoma (Figure 4B); however, some areas of the lesion showed sparse cellularity and rarefied interstitial tissue. Based on these histopathologic findings, the tumor was diagnosed as a primary mesenchymal chondrosarcoma.

After 6 months of operation, the patient underwent abdominal and pelvic CT, and no recurrence or metastasis was found in any abdominal organ (Figure 5).

## 3. Discussion

Primary retroperitoneal ESMC is a rare and aggressive malignancy and shows a poor prognosis (5, 6). The etiology of ESMC has not been fully elucidated; however, some studies have found that the chromosomal translocation might

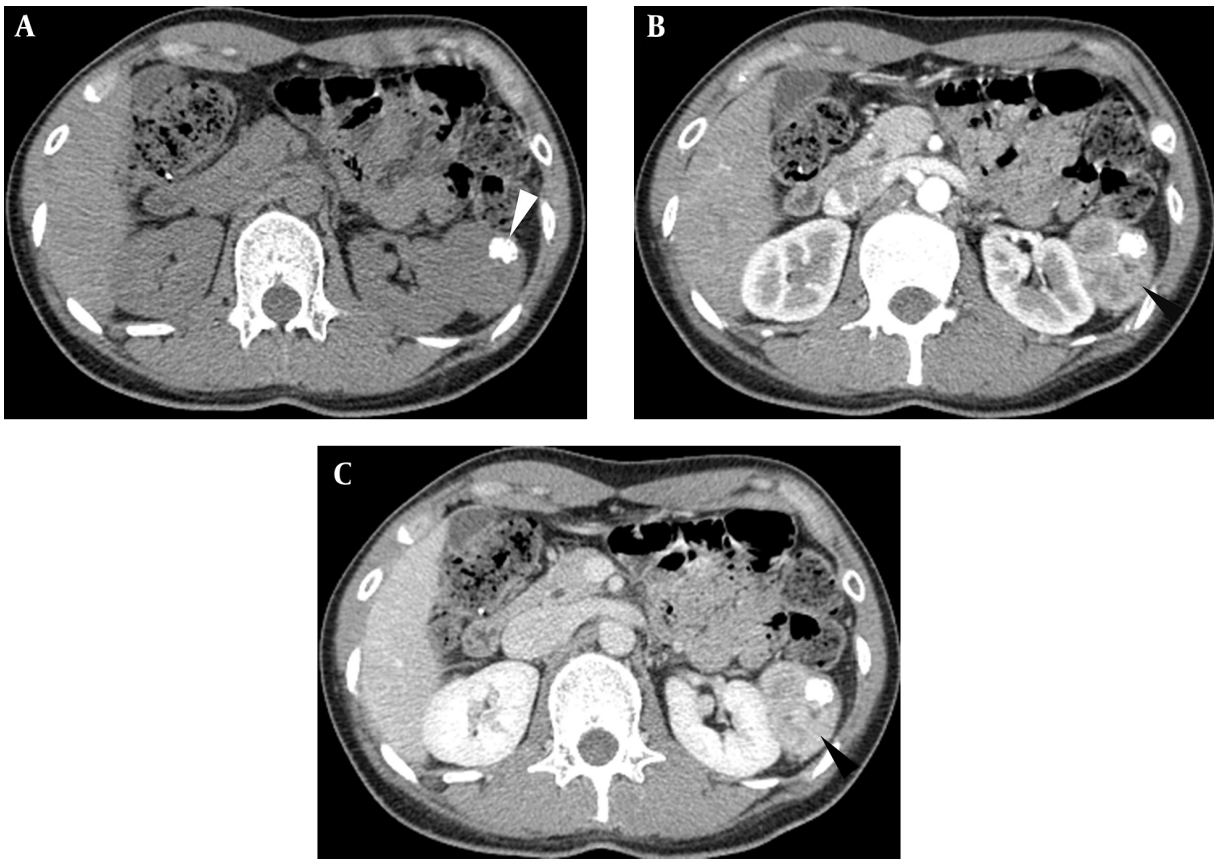


**Figure 2.** Axial CT images. A, Homogeneous iso-attenuation mass with nodular calcification (white arrowhead) is detected on plain scan; B, Parenchyma of the mass shows enhancement (black arrowhead) in the arterial phase and C, Vivid enhancement (black arrowhead) in the portal phase.

play an important role in its pathogenesis, although the precise molecular mechanism was not identified (7).

Histologically, ESMC has a typical pattern consisting of both primitive small spindle-shaped mesenchymal cells with a very dense distribution and well-defined islands of cartilaginous tissue. In addition, dilated vascular channels in the mass resemble hemangiopericytomas (8, 9).

Mesenchymal chondrosarcoma generally occurs in the 2nd and 3rd decades of life (6), and most patients show nonspecific symptoms except for pain and swelling and epigastric discomfort. Early and accurately diagnosing or prompting the probability of this tumor is significant for making treatment protocols and the operational plan. Imaging examinations such as CT, MRI, and ultrasonography play an important role in diagnosing and evaluating this malignant tumor.

Abdominal enhancement CT is a useful examination to diagnose and evaluate retroperitoneal tumors, especially for tumors that contain calcium foci. Previous studies have indicated that a large soft-tissue mass with extensive ring- and arc-like calcific foci is a typical imaging feature of primary ESMC (1, 4), as well as slight heterogeneous enhancement in the periphery of the mass and no evident enhancement in most of the mass (4). However, in our case, gross, nodule-like calcification was evident in the lesion, and a significant and gradual enhancement pattern in the parenchymal and inner hypoattenuation foci was observed. Biphasic enhanced CT may provide more useful imaging information regarding the blood supply of primary ESMC. We believe this enhancement pattern is consistent with the abundant dilated vascular channel in the mass. Moreover, a different proportion of the parenchyma component to the calcific area induces different imaging features; the majority of features in this case of primary ESMC contain neoplasm parenchyma, which is significantly different than previously reported cases.

MRI examination is more sensitive to explore the inner components of tumors, and DWI is a very helpful imaging method to evaluate cellularity in the mass by observing water molecular diffusion. In this case, most of the

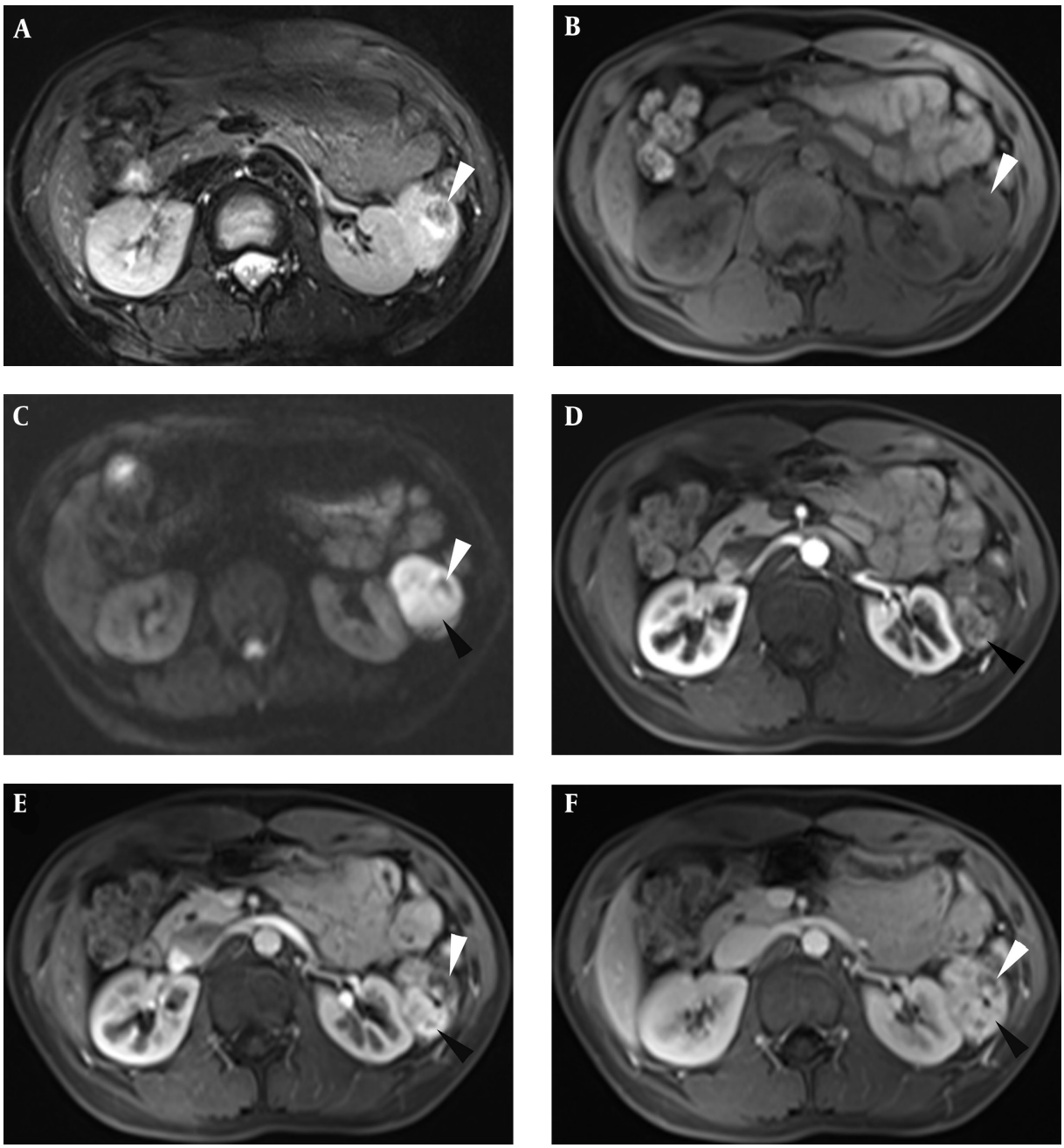


**Figure 3.** MRI images showing the lesion was heterogeneous hyperintense with nodular hypointense calcium foci (white arrowhead) on T2 weighted image (T2WI) (A), iso-hypointensity with hypointense calcification (white arrowhead) on T1 weighted image (T1WI) (B), and hyperintensity with hypointense calcification on diffusion-weighed imaging (DWI) (C); the parenchyma of the mass showed quick enhancement (black arrowhead) in the arterial phase (D) and vivid enhancement (black arrowhead) in the portal phase (E), along with contrast agent wash out (black arrowhead) in the equilibrium phase (F); the edge of the calcific area showed centrality enhancement (white arrowhead) in the portal phase and equilibrium phase (E and F).

parenchyma in the lesion showed heterogeneous hyperintensity on T2WI and iso-hypointensity on T1WI. Particularly, the mass indicated hyperintensity on DWI and hypointensity on the ADC map. These MRI features imply the dense cellularity of tumor cells, consistent with our pathological findings. Multiphase contrast-enhanced MRI is more detailed than biphasic enhanced CT and dynamically shows the vivid enhancement degree and wash-in-

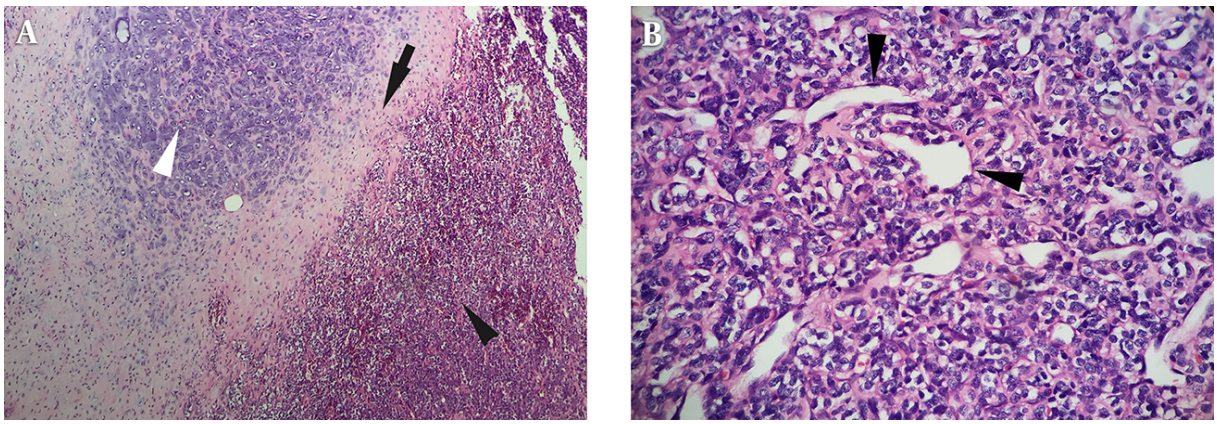


**Figure 4.** Microscopic examination confirmed the cartilaginous tissue area (white arrowhead) surrounded with dense hyperchromatic cellularity (black arrowhead) and a transition belt of two components (black arrow) (A) (H&E staining, × 100); the neoplastic cells are arranged similar to those in hemangiopericytoma (black arrowheads) (B) (× 400)

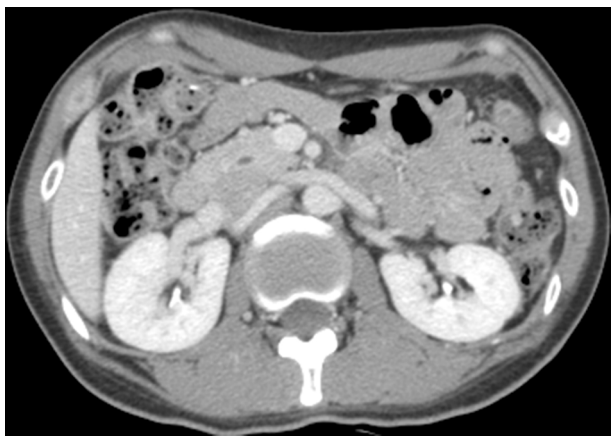

**Figure 5.** Axial CT image indicated no tumor recurrence in the left perirenal space, after 6 months of the operation.

wash-out enhancement pattern of primary ESMC, representing an abundant blood supply. Nodular calcification was hypointense in the interior of the mass on T1WI, T2WI and DWI. Similar to some previous reports, heterogeneous enhancement within calcified areas in the lesion of primary ESMC was seen in the orbit (9) or limb (7, 10). In our case, the calcific area showed moderate centrality enhancement in the equilibrium phase. However, we presume that the enhancement area in the so-called calcific area may be the transfer area containing cartilage and parenchyma cells with neoplasm blood vessels based on the histopathologic features in this primary ESMC.

Retroperitoneal primary ESMC is necessarily differentiated from common retroperitoneal tumors, including schwannoma, solitary fibrous tumor, and Castleman disease. Schwannoma typically appears with mucinous degeneration or large necrosis areas, indicated as hypoattenuation on CT and hyperintensity on T2WI and hypointensity on T1WI, and these tumors seldom contain calcium foci or small granular calcifications (11), a finding that is more different than that in the retroperitoneal primary ESMC. Because of dense cellularity in the primary ESMC, the DWI signal of neoplasm parenchyma is higher than that in schwannoma. On CT and MRI, the common appearances of both the solitary fibrous tumor and Castleman disease are well-defined masses with evident enhancement (12). These imaging features are similar to our case of primary ESMC. However, Castleman disease usually shows a homogeneous solitary mass surrounded by small satellite nodules, and both solitary fibrous tumors and Castleman disease show no evident calcification in the lesions. These imaging characteristics may be helpful in differentiating primary ESMC from Castleman disease.

In addition to marked calcification in the well-circumscribed mass, primary ESMC in the retroperitoneum may appear as significant enhancement with a gradual enhancement pattern on biphasic enhanced CT and a wash-in-wash-out enhancement pattern on multiphase contrast-enhanced MRI. Due to the dense cellularity of the parenchyma resulting in hydrogen diffusion-hindering obstacles, the mass shows hyperintensity on DWI. We present the imaging features of this new case of primary ESMC to enrich the imaging knowledge of this tumor and look forward to providing valuable imaging information to diagnose and differentiate primary ESMC from common retroperitoneal tumors; however, additional study is necessary to explore the imaging

characteristics of this tumor.

## Footnotes

**Authors' Contributions:** The authors were involved in acquisition of data, analysis and interpretation of data, drafting of the manuscript, critical revision of the manuscript for important intellectual content, statistical analysis, technical, and material support of this study. Guyi Wang and Zhenhua Zhao contributed equally to this study.

**Financial Disclosure:** None declared.

**Funding/Support:** This study was supported by research grants from Research Projects of Public Technology Application of Science and Technology of Shaoxing City (2013B70080, 2015B70065).

## References

1. Taori K, Patil P, Attarde V, Chandanshive S, Rangankar V, Rewatkar N. Primary retroperitoneal extraskeletal mesenchymal chondrosarcoma: a computed tomography diagnosis. *Br J Radiol*. 2007;**80**(959):e268–70. doi: 10.1259/bjr/13711118. [PubMed: 17989325].
2. D'Andrea G, Caroli E, Capponi MG, Scicchitano F, Osti MF, Bellotti C, et al. Retroperitoneal mesenchymal chondrosarcoma mimicking a large retroperitoneal sacral schwannoma. *Neurosurg Rev*. 2008;**31**(2):225–9. doi: 10.1007/s10143-007-0106-4. [PubMed: 17912561].
3. White DW, Ly JQ, Beall DP, McMillan MD, McDermott JH. Extraskeletal mesenchymal chondrosarcoma: case report. *Clin Imaging*. 2003;**27**(3):187–90. [PubMed: 12727057].
4. Hu HJ, Liao MY, Xu LY. Primary retroperitoneal extraskeletal mesenchymal chondrosarcoma involving the vena cava: A case report. *Oncol Lett*. 2014;**7**(6):1970–4. doi: 10.3892/ol.2014.2012. [PubMed: 24932271]. [PubMed Central: PMC4049765].
5. Oh BG, Han YH, Lee BH, Kim SY, Hwang YJ, Seo JW, et al. Primary extraskeletal mesenchymal chondrosarcoma arising from the pancreas. *Korean J Radiol*. 2007;**8**(6):541–4. doi: 10.3348/kjr.2007.8.6.541. [PubMed: 18071285]. [PubMed Central: PMC2627457].
6. Varma DG, Ayala AG, Carrasco CH, Guo SQ, Kumar R, Edeiken J. Chondrosarcoma: MR imaging with pathologic correlation. *Radiographics*. 1992;**12**(4):687–704. doi: 10.1148/radiographics.12.4.1636034. [PubMed: 1636034].
7. Hashimoto N, Ueda T, Joyama S, Araki N, Beppu Y, Tatezaki S, et al. Extraskeletal mesenchymal chondrosarcoma: an imaging review of ten new patients. *Skeletal Radiol*. 2005;**34**(12):785–92. doi: 10.1007/s00256-005-0025-9. [PubMed: 16211384].
8. Xu J, Li D, Xie L, Tang S, Guo W. Mesenchymal chondrosarcoma of bone and soft tissue: a systematic review of 107 patients in the past 20 years. *PLoS One*. 2015;**10**(4). e0122216. doi: 10.1371/journal.pone.0122216. [PubMed: 25849226]. [PubMed Central: PMC4388572].
9. Shinaver CN, Mafee MF, Choi KH. MRI of mesenchymal chondrosarcoma of the orbit: case report and review of the literature. *Neuroradiology*. 1997;**39**(4):296–301. [PubMed: 9144681].
10. Chen Y, Wang X, Guo L, Li Y, Deng S, Liu Y, et al. Radiological features and pathology of extraskeletal mesenchymal chondrosarcoma. *Clin Imaging*. 2012;**36**(4):365–70. doi: 10.1016/j.clinimag.2011.11.001. [PubMed: 22726976].
11. Liu QY, Lin XF, Zhang WD, Li HG, Gao M. Retroperitoneal schwannomas in the anterior pararenal space: dynamic enhanced multislice CT and MR findings. *Abdom Imaging*. 2013;**38**(1):201–10. doi: 10.1007/s00261-012-9882-6. [PubMed: 22484919].
12. Zhou LP, Zhang B, Peng WJ, Yang WT, Guan YB, Zhou KR. Imaging findings of Castleman disease of the abdomen and pelvis. *Abdom Imaging*. 2008;**33**(4):482–8. doi: 10.1007/s00261-007-9282-5. [PubMed: 17624567].